

Variable stability in-flight simulation system based on existing autopilot hardware

Scholten, Pepijn A.; van Paassen, Marinus M.; Chu, Q. Ping; Mulder, Max

DOI

[10.2514/1.G005066](https://doi.org/10.2514/1.G005066)

Publication date

2020

Document Version

Accepted author manuscript

Published in

Journal of Guidance, Control, and Dynamics

Citation (APA)

Scholten, P. A., van Paassen, M. M., Chu, Q. P., & Mulder, M. (2020). Variable stability in-flight simulation system based on existing autopilot hardware. *Journal of Guidance, Control, and Dynamics*, 43(12), 2275-2288. <https://doi.org/10.2514/1.G005066>

Important note

To cite this publication, please use the final published version (if applicable). Please check the document version above.

Copyright

Other than for strictly personal use, it is not permitted to download, forward or distribute the text or part of it, without the consent of the author(s) and/or copyright holder(s), unless the work is under an open content license such as Creative Commons.

Takedown policy

Please contact us and provide details if you believe this document breaches copyrights. We will remove access to the work immediately and investigate your claim.

A Variable Stability In-Flight Simulation System based on existing Autopilot Hardware

Pepijn A. Scholten*, Marinus M. van Paassen[†], Q. Ping Chu[‡] and Max Mulder[‡]

Delft University of Technology, 2629 Delft, The Netherlands

A variable stability in-flight simulator has the capabilities to change the response of an aircraft in-flight, often without changing the physical properties of the aircraft. The ability to adjust the aircraft response characteristics and handling qualities has various purposes, such as pilot training, control system development and handling quality research. A variable stability control system is designed for a medium range business jet using Incremental Non-linear Dynamic Inversion. The performance of the in-flight simulator is verified by two experiments, one conducted in a fixed-base flight simulator and one in a Cessna Citation II laboratory aircraft. The fly-by-wire actuation system in the Cessna Citation II is based on its existing autopilot, inheriting the limited performance and safety protections. The simulator experiment shows differences between the experienced handling qualities for a reference model and the designed controller combined with aircraft dynamics. These differences mainly arise due to actuator saturation for specific handling quality settings. The in-flight experiment supports the simulator findings but also reveals how the available control authority around the initial condition is limited due to constraints of the fly-by-wire system.

Nomenclature

α	= Angle of attack [<i>rad</i>]
β	= Side slip angle [<i>rad</i>]
δ_a, δ_e	= Aileron, elevator deflection [<i>rad</i>]
$\dot{\phi}, \dot{\theta}$	= Roll, pitch rate [<i>rad/s</i>]
ω	= Angular acceleration [<i>rad/s</i> ²]
ω_c	= Crossover frequency [<i>rad/s</i>]
ω_p, ω_q	= Roll, pitch natural frequency [<i>rad/s</i>]
ω_{sp}	= Aircraft short period natural frequency [<i>rad/s</i>]
\bar{c}	= Mean aerodynamic chord [<i>m</i>]
ϕ, θ	= Roll, pitch angle [<i>rad</i>]
ρ	= Air density [<i>kg/m</i> ³]
ζ_p, ζ_q	= Roll, pitch damping ratio
ζ_{sp}	= Aircraft short period damping ratio

b	= Wing span [m]
C_*	= Aircraft dynamic coefficients
J	= Inertia tensor
K_*	= Control gains
M_a	= Moment induced by the airframe [Nm]
M_c	= Moment induced by the control effectors [Nm]
M_T	= Moment induced by thrust [Nm]
$n_{z,ss}$	= Normal steady state acceleration [m/s]
p, q, r	= Roll, pitch and yaw rate [rad/s]
S	= Wing surface area [m^2]
T_{θ_2}	= Longitudinal pitch response coefficient [s]
u, u_p	= Input and pilot input
u_{mod}	= Modified input after reference model
u_{req}	= Requested input after side stick gains [rad]
V	= Airspeed [m/s]
v_h	= Hedging signal
V_{ias}	= Indicated airspeed [m/s]
V_{tas}	= True airspeed [m/s]
x	= Aircraft states
CAP	= Control Anticipation Parameter
DUECA	= Delft University Environment for Communication and Activation
FAST	= Full-scale Advanced System Testbed
FL	= Flight Level
HMI Lab	= Human Machine Interaction Laboratory
HOS	= High Order System
IMU	= Inertial Measurement Unit
INDI	= Incremental Non-linear Dynamic Inversion
LOES	= Low Order Equivalent System
NASA	= National Aeronautics and Space Administration
NLR	= Netherlands Aerospace Centre
PCH	= Pseudo-Control Hedging
PID	= Proportional Integral Derivative
PIO	= Pilot Induced Oscillations

I. Introduction

*

Training of test pilots requires them to experience a variation of handling qualities. Multiple different aircraft would be required to provide these handling qualities, significantly increasing training costs. A variable stability in-flight simulator is a system which has the capabilities to change the response of an aircraft *in-flight*, often without changing the physical properties of the aircraft, allowing adjustments of response characteristics and handling qualities. An aircraft equipped with such a system can mimic the response of other aircraft, also during flight. Apart from training benefits, such a system can also be used for control law development and handling quality research [1].

In the early years, variable stability simulators were used to design control systems for different flight situations, like landing on an aircraft carrier [2, Ch. 2]. In the 1970s and 1980s, focus moved from specific flight situations or aircraft configurations to testing conceptual control systems of novel aircraft. More recent developments show the possibility for the in-flight simulator to follow the dynamics of different aircraft [2, Ch. 5].

Different methods have been investigated to modify the handling qualities using variable stability. The response feedback method, is a basic method that feeds back the aircraft response to modify the control inputs, Mirza et al. [3]. This method enables modification of the handling qualities, but does not offer direct selection. More advanced methods, which enable selection of handling qualities, use a reference model for the desired dynamics. The aircraft's responses can then be forced to follow the reference model by model-following [4], [5] [6]. A drawback of both methods is that multiple linear controllers are required, and since an aircraft is a non-linear system, these controllers have to be gain-scheduled in the operating regime of the aircraft, requiring considerable tuning effort. As an alternative to using a model-following control law, the control actions can also be determined by inverse control, where an inverse model of host aircraft is used to determine the required control inputs.

The non-linearities can also be accounted for by using dynamic inversion, a method that uses the differentiation of the aircraft output until the control input appears in the derivative [7, Ch. 6]. Ko et al. [8] developed a variable stability system based on this principle, where the pitch, roll, yaw and normal load could be matched [9]. Their research was limited to offline simulations and linearized aircraft models. Miller [10] introduced non-linear aircraft models and flew the variable stability system in a modified F-18. This implementation required full non-linear aircraft models and is thus constrained by the availability and accuracy of these models.

Incremental non-linear dynamic inversion (INDI) is a development in the field of dynamic inversion that can eliminate the need for a full non-linear aircraft model. INDI uses the measured aircraft accelerations and converts these to equivalent pitch, roll or yaw inputs with a moment effectiveness parameter [11]. Germann [12] designed a variable stability system using INDI for the T-6A Texan II aircraft. He linearized the moment effectiveness parameter which limited the performance of his system and he only tested the system in offline simulation. Grondman et al. [13] developed an INDI controller for the Cessna Citation II laboratory aircraft. Their controller was flown successfully but was not designed for variable stability.

*Researcher, Control and Simulation, Faculty of Aerospace Engineering, Kluyverweg 1; p.a.scholten@live.nl

†Associate Professor, Control and Simulation, Faculty of Aerospace Engineering, Kluyverweg 1; m.m.vanpaassen@tudelft.nl. Member AIAA

‡Associate Professor, Control and Simulation, Faculty of Aerospace Engineering, Kluyverweg 1; q.p.chu@tudelft.nl. Member AIAA

‡Professor, Control and Simulation, Faculty of Aerospace Engineering, Kluyverweg 1; m.mulder@tudelft.nl. Associate Fellow AIAA

*A part of the work described in this paper was presented at the AIAA Scitech 2020 Forum, Orlando, Jan 6-10, 2020, as paper no. AIAA 2020-0852

This paper presents a design for a variable stability in-flight simulator using off-the-shelf hardware, employing INDI for the inner loop. The system was tested in offline simulation, a simulator experiment and in the Cessna Citation II laboratory aircraft operated by TU Delft and NLR. The limits of this system were investigated. The fly-by-wire actuation system in the Cessna Citation II is based on its existing autopilot, inheriting the limited performance and safety protections [14, 15]. The control authority of the autopilot is restricted due to limitations in torque which are imposed on the actuator servo motors. Hence, the proposed system is expected to be limited by accuracy of the moment effectiveness and performance of the actuation system, and determining how these system limitations propagate to the variable stability system is one of the main purposes of this research.

The paper is structured as follows. First, additional background information is presented in Section II. Second, the controller design is explained in Section III. The controller is tested in offline simulations in Section IV, in a flight simulator experiment in Section V and validated in real flight tests in Section VI. The paper ends with a discussion and conclusions.

II. Background

A. Variable Stability

1. Response feedback

Response feedback is the most basic method to achieve a variable stability system. The response output of the aircraft is measured and fed back to modify the control inputs. A mathematical description of this system is given by Nelson [16, Ch. 10] and the solution technique for achieving a target response, using the Riccati equations, is presented by Bryson and Ho [17, Ch. 14]. Mirza et al. [3] found that response feedback is effective in changing the stability and handling qualities. Handling qualities that are changed by response feedback could be identified by the pilots in their experiment, even in a fixed-base simulation.

2. Model-following

A second method to achieve a variable stability system is model-following. The aircraft response is changed so it performs like a predetermined model, offering benefits when designing aircraft to meet the specifications determined by regulations. Two different strategies, implicit or explicit model-following, are used to design model-following control systems, as originally described by Armstrong [4], O'Brien and Broussard [5] and Kreindler and Rothschild [6]. The implicit model-following technique is a basic method where gains are selected to reach the desired behavior. In explicit model-following, the model to be followed is placed inside the control system, generating reference behavior.

B. Control methods

In a response feedback system, the control is coupled with the variable stability system. For explicit model-following systems, a separate control law is needed for the inner loop. This can be a closed-loop control law, but for their apparent advantages, dynamic inversion techniques are considered here.

1. *Dynamic inversion*

The previously presented control methods share the same drawback. Since an aircraft is a non-linear system, the described design tools require multiple linear controllers, which have to be gain-scheduled in the operating regime of the aircraft. Alternatively, these non-linearities can be accounted for with a technique called *dynamic inversion*. Slotine and Li [7] developed the initial concept, which uses differentiation of the output until the control input appears in the derivative.

Such a linear dynamic inversion was implemented by Ko et al. [8] in a variable stability system. They used a model of the Korean next-generation fighter and used linear dynamic inversion to follow the dynamics of the F-16 fighter aircraft in offline simulations. Ko and Park [18] introduced an updated version of their system, which included a switching mechanism between the normal flight computer and the dynamic inversion model. Finally Ko and Park [9] introduced the normal load to their initial variable stability control system, that only could follow pitch, roll and yaw. However, they do not discuss the main limitation of linear dynamic inversion. The performance of the linear dynamic inversion is constrained by the performance of the linear model of the aircraft. The linear model, in turn, depends on both the accuracy of the model and the operating point where it is linearized.

Non-linear dynamic inversion solves some of these issues by using a model of the aircraft non-linear dynamics, in contrast to the previously used linear approximation. In practice, full look-up tables have to be implemented in the controller. Miller [10] shows such an implementation for the FAST system from NASA, with hardware in the loop simulation experiments. However, recent developments within dynamic inversion provide a means to avoid the requirement of a full non-linear model of the aircraft.

2. *Incremental non-linear dynamic inversion*

Incremental non-linear dynamic inversion (INDI) uses the advantages from the dynamic inversion, but does not require the full non-linear aircraft model. The development of INDI can be traced back to Smith [11]. He acknowledges the issues with the non-linear dynamic inversion and proposes a new method using acceleration sensors. The accelerations are converted to an equivalent pitch, roll or yaw input using a moment effectiveness parameter (based on the moment due to control surface deflection and the aircraft inertia). He demonstrated the INDI method provides considerable robustness regarding authority limits, sensor noise and significant variations within the control law (mainly inertia and control powers).

The combination of the actuator position sensor and the acceleration sensors ensure angular accelerations are matched robustly. Germann [12] developed a variable stability system for the T-6A Texan II for the US Air Force based on INDI. He showed in offline simulations that the Texan II matches the dynamics of the F-16 aircraft. Bacon and Ostroff [19] used the INDI method to design a re-configurable flight control system in case of system failure. They acquired the angular accelerations by combining linear accelerations and differentiating the angular rates. This created noise and was considered to be sufficient but not optimal since the differentiation also introduced some time delays. Cox and Cotting [20] continued the development of the ideas from Smith, Bacon and Ostroff. They implemented INDI in the ground-based simulators at NASA Dryden. The main takeaway from their work is that INDI is viable for real-time aircraft control and simulation, not just in an offline simulation.

Smeur et al. [21, 22] showed the INDI controller to perform better regarding gust resistance, compared to a normal Proportional Integral Derivative (PID) controller. Grondman et al. [13], Keijzer et al. [23] worked on INDI control for the Cessna Citation II,

which was based on angular rate control. These controllers were flown successfully in the Cessna Citation II, but provided inner loop stabilization, and was not used for variable stability.

C. Handling Qualities

Handling qualities are defined as “*those qualities or characteristics of an aircraft that govern the ease and precision with which a pilot is able to perform the tasks required in support of an aircraft role*” [24]. This definition shows a clear combination of performance of the pilot and the aircraft acting together as a system for specific maneuvers of the aircraft.

1. Control Anticipation Parameter

The Control Anticipation Parameter (CAP) is a longitudinal handling quality criterion which focuses on the short period pitch aircraft response. CAP was originally introduced by Bihle [25], after which it became one of the criteria to measure longitudinal handling qualities, defined in the MIL-STD-1797A, Flying Qualities of Piloted Aircraft [26]. CAP is expressed as the ratio of initial pitch acceleration (second derivative of θ) to the normal acceleration in steady state $n_{z_{ss}}$:

$$CAP = \frac{\ddot{\theta}(0)}{n_{z_{ss}}} \quad (1)$$

Bischoff [27] argued the CAP can be calculated from the short period characteristics of the aircraft. This method only holds for aircraft with a general second-order longitudinal response as given in:

$$\frac{q}{\delta_e} = \frac{K_\theta(s + \frac{1}{T_{\theta_2}})}{s^2 + 2\zeta_{sp}\omega_{sp}s + \omega_{sp}^2} \quad (2)$$

Based on this assumption, Bischoff rewrites Equation 1 to:

$$CAP \approx \frac{\omega_{n_{sp}}^2}{n/\alpha} \approx \frac{\omega_{n_{sp}}^2}{\frac{V}{g} \frac{1}{T_{\theta_2}}} \quad (3)$$

When the CAP is used as a handling quality criterion, it is always indicated in combination with the short period damping ratio. This criterion is categorized into different flight phases (A, B, C) and aircraft classes (I, II, III, IV). Within these categories, another segmentation exists into three different levels of acceptability (Level 1, 2 and 3).

- Level 1: Flying qualities are adequate for mission flight,
- Level 2: Flying qualities are adequate to accomplish the mission with increased pilot workload, and
- Level 3: Flying qualities cause inadequate mission effectiveness due to excessive pilot workload.

2. Low Order Equivalent System

The combined actuator and aircraft dynamics are of higher order compared to the second-order longitudinal response as assumed by Bischoff. Di Franco [28] was one of the first to research the effects of Higher Order System (HOS) dynamics on the longitudinal handling qualities. He determined the aircraft short period response could be represented by a second-order equivalent term and a time delay. This was further developed into the Low Order Equivalent System (LOES) concept by Hodgkinson et al. [29]. They created an equivalent low order system by matching the complex frequency response of the higher order systems. In this way, a HOS can be represented as a low order system with a time delay term, and analytical methods developed for low order systems can be applied.

There are several techniques available to determine the LOES and their advantages and disadvantages are discussed by Mirza et al. [3]. The most robust method is the *Output Error* and *Equation Error* approach developed by Morelli [30]. The LOES method uses the equation error and output error parameter estimation in the frequency domain. They are two separate parameter estimation methods. The equation error method can estimate the parameters by fixing the time delay to a specific initial condition, whereas the output error method requires initial estimates for all parameters. However, the equation error method does not guarantee a global minimum. That is why Morelli suggested using the parameters from an initial equation error estimation as a guess for the output error estimation. This results in the estimation with the lowest error.

3. Cooper-Harper Rating

The Cooper-Harper rating scale is one of the accepted standards for subjective handling quality measurement. Cooper and Harper [24] developed a decision tree rating scale as a tool to assess aircraft handling quality. The scale takes qualitative pilot comments and translates them into a quantitative scale from 1 to 10, and can be used in experiments to find the handling qualities as experienced by the pilots.

III. Controller Design

A. Requirements and overall design

Several requirements for this controller were determined. Primarily, the controller should allow for accurate tracking of the CAP reference model. Since the capability of the chosen actuators is limited, the controller should achieve good performance with the limited system and properly handle situations with actuator saturation.

In addition, the implementation of the controller should be flexible, since that the variable stability platform should be suitable for multiple in-flight simulation purposes. This implies it can be used for multiple goals without having to change the basic logic. To enable this, an architecture with **inner loop** and **outer loop** have been defined, where the functionality of the inner loop is independent of the outer loop. The outer loop can be used to define the different control goals.

The actuator limitations are also introduced in the simulator model, enabling the simulator experiment to give an indication of the performance of the in-flight simulator.

In order to achieve the required flexibility, a structure with an explicit CAP reference model is used. An optimal use of the limited actuator capabilities are ensured by an INDI-based inner loop controller, and Pseudo-control hedging is applied for to prevent controller saturation when the capability of the actuators is insufficient. The experimental controller aircraft does currently not have a means for yaw control inputs, and a side-slip controller is used to ensure coordinated flight. The schematic block diagram of the controller structure is shown in Figure 1.

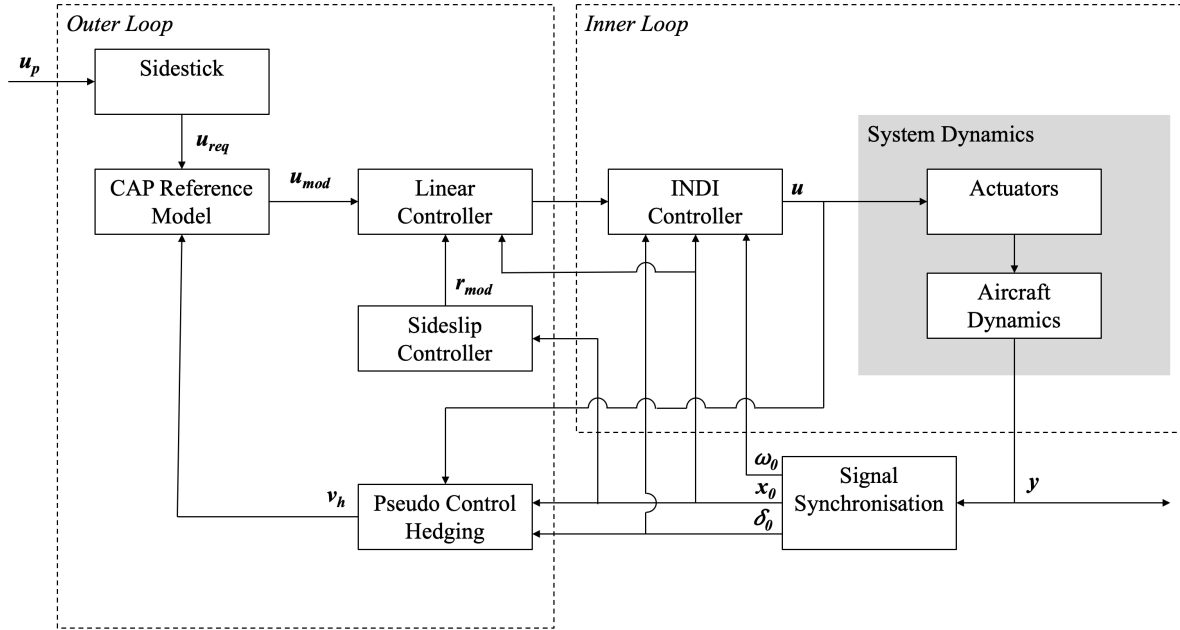


Fig. 1 Schematic block diagram of the controller structure

B. Outer Loop

1. Sideslip Controller

The Cessna Citation II fly-by-wire hardware does not include a yaw input device, which means coordinated flight can only be achieved when the side slip is controlled. This has been recognized by Grondman et al. [13], who developed a PI controller to control the side slip to zero. This is described in the following equation, where $K_\beta = 1.93$, $K_{\beta_I} = 0.977$ and $w = V_{tas} \sin \alpha \approx V_{tas} \alpha$:

$$r_{mod} = \frac{1}{V_{tas}} (wp - f_y) \left(\frac{1}{s} K_{\beta_I} (\beta_{cmd} - \beta) - K_\beta \beta \right) \quad (4)$$

2. CAP Reference Model

The CAP reference model in pitching motion is designed to ensure a requested CAP and damping using the second-order approximation as determined by Bischoff [27]. The linear controller uses u_{mod} as an input, which is essentially a reference pitch and roll rate. Yaw is not controlled to zero by the controller, thus it is not present in the CAP reference model. To convert the

requested input u_{req} to these reference rates, an estimation of both the pitch gain K_θ and the longitudinal coefficient T_{θ_2} are required as given in Equation 2. To achieve this estimation, the method from Morelli [30] is used. Since the CAP and damping are design parameters, Equation 2 can be rewritten to provide the final CAP reference model:

$$\frac{u_{mod_q}}{u_{req_q}} = \frac{a_1 s + a_2}{s^2 + b_1 s + b_2} \quad (5)$$

The corresponding coefficients are:

$$\begin{aligned} a_1 &= K_\theta & a_2 &= \frac{K_\theta}{T_{\theta_2}} \\ b_1 &= 2\zeta_q \sqrt{\text{CAP} \cdot \frac{V}{g} \frac{1}{T_{\theta_2}}} & b_2 &= \frac{\text{CAP} V}{T_{\theta_2} g} \end{aligned} \quad (6)$$

The reference model unfortunately included an erroneous implementation of the roll dynamics. The implemented dynamics were stable, so that the wings were kept level during the experiments, and the deficiency did not interfere with longitudinal motion.

3. Control gain scaling

The inputs from the pilot have to be scaled before they can enter the controller. Since both roll and pitch axes have different reference model, they need different gains. The initial values were determined using a pilot model, where the gain was changed until the open loop crossover frequency ω_c was equal to 2 [rad/s]. This led to the following standard stick gains: Pitch $K_q = 0.0125$ and roll $K_p = 0.65$.

4. Linear Controller

The linear controller was designed to follow the reference model as closely as possible. For the pitch and roll channel, the error for the state and the first derivative are controlled. In addition, a feed-forward gain is added for the second derivative. The result can be seen in the following Equations:

$$v_{\dot{\phi}} = \left(K_\phi + \frac{K_{\phi_I}}{s} \right) (u_{mod_p} - \phi) + K_{\dot{\phi}} (\dot{u}_{mod_p} - \dot{\phi}) + K_{\ddot{\phi}} \ddot{u}_{mod_p} \quad (7)$$

$$v_{\dot{\theta}} = \left(K_\theta + \frac{K_{\theta_I}}{s} \right) (u_{mod_q} - \theta) + K_{\dot{\theta}} (\dot{u}_{mod_q} - \dot{\theta}) + K_{\ddot{\theta}} \ddot{u}_{mod_q} \quad (8)$$

Side slip is controlled in the yaw channel, without any pilot input:

$$v_r = K_r (r_{mod} - r) \quad (9)$$

Grondman et al. [13] performed a robust parameter synthesis to optimize these gains. However, their design requirements were different, since they did not require exact model-following. A linear parameter grid search was performed to find the combination of gains that enabled better model-following performance. The results of this analysis are summarized in Table 1.

Table 1 Linear controller gains

<i>Roll</i>		<i>Pitch</i>	
K_ϕ	5.51	K_θ	7.76
K_{ϕ_I}	1.34	K_{θ_I}	0.50
$K_{\dot{\phi}}$	4.80	$K_{\dot{\theta}}$	4.80
$K_{\ddot{\phi}}$	1.05	$K_{\ddot{\theta}}$	0.70
<i>Yaw</i>			
K_r	1.62		

5. Pseudo-Control Hedging

Johnson and Calise [31] developed the Pseudo Control Hedging (PCH) technique to compensate for actuator limitations by modifying the reference model dynamics. PCH is implemented in the controller to compensate for actuator saturation, which is expected due to the limited fly-by-wire system performance. This requires the inverse of the moment effectiveness matrix to correct for the differences between the commanded deflection by the inner loop INDI controller and the actual deflection of the actuators, providing the hedging signal as indicated in:

$$v_h = M_c J^{-1}(u - \delta_0) \tag{10}$$

Lombaerts and Looye [32] activated the PCH only when saturation occurred, whilst Grondman et al. [13] always kept the PCH active. In the latter case, the reference signal is also corrected for limited actuator speed instead of only the actuator position and this option is therefore preferred.

C. Inner Loop

1. INDI

Non-linear dynamic inversion allows tight tracking of the reference signal without a need for large inner loop gains that a feedback-based model following system would require[10]. Over that, a large benefit of the INDI method is that the INDI controller uses information from the system dynamics to adapt the moment effectiveness dependent on the flight condition, eliminating the need for full inversion of a non-linear dynamic model[12]. In this way, parts of the aerodynamic moment M_A can be neglected in the model, and it is expected that the controller can effectively use the limited actuator capabilities. The aerodynamic moment can be split into three main components: The moment induced by thrust M_T ; the moment induced by the control effectors M_c and the airframe dependent moment M_a .

It is assumed the moment induced by the thrust can be neglected, $M_T \approx 0$. The airframe dependent moment and the moment

induced by the control effectors are described by the following equations:

$$\mathbf{M}_a = \frac{1}{2} \rho V_{tas}^2 S \begin{bmatrix} bC_{l_a} \\ \bar{c}C_{m_a} \\ bC_{n_a} \end{bmatrix} \quad (11)$$

$$\mathbf{M}_c = \frac{1}{2} \rho V_{tas}^2 S \begin{bmatrix} bC_{l_{\delta a}} & 0 & bC_{l_{\delta r}} \\ 0 & \bar{c}C_{m_{\delta e}} & 0 \\ bC_{n_{\delta a}} & 0 & bC_{n_{\delta r}} \end{bmatrix} \quad (12)$$

In these equations, V_{tas} is the true airspeed, ρ is the air density, b is the wing span, \bar{c} is the mean aerodynamic chord, S is the wing surface area and C_* are the aircraft's dynamic coefficients. These dynamic coefficients are defined by the system dynamics and retrieved from the aircraft model. Equations 11 and 12 can be incorporated in the rotational dynamics of rigid-body aircraft over a flat non-rotating earth as given in the Newton-Euler equation:

$$\dot{\boldsymbol{\omega}} = \mathbf{J}^{-1}(\mathbf{M}_A + \mathbf{M}_T - \boldsymbol{\omega} \times \mathbf{J}\boldsymbol{\omega}) \quad (13)$$

Here \mathbf{J} is the inertia tensor as given in:

$$\mathbf{J} = \begin{bmatrix} I_{xx} & 0 & -I_{xz} \\ 0 & I_{yy} & 0 \\ -I_{xz} & 0 & I_{zz} \end{bmatrix} \quad (14)$$

This leads to the following result:

$$\dot{\boldsymbol{\omega}} = \mathbf{J}^{-1}(\mathbf{M}_a + \mathbf{M}_c \mathbf{u} - \boldsymbol{\omega} \times \mathbf{J}\boldsymbol{\omega}) \quad (15)$$

The control law for INDI is obtained by taking a first-order Taylor expansion around the current point in time, which is denoted by the subscript 0. This Taylor expansion can be found in:

$$\dot{\boldsymbol{\omega}} \approx \dot{\boldsymbol{\omega}}_0 + \frac{\partial}{\partial \boldsymbol{\omega}} \left(\mathbf{J}^{-1}(\mathbf{M}_a + \mathbf{M}_c \mathbf{u} - \boldsymbol{\omega} \times \mathbf{J}\boldsymbol{\omega}) \right) (\boldsymbol{\omega} - \boldsymbol{\omega}_0) + \frac{\partial}{\partial \mathbf{u}} \left(\mathbf{J}^{-1}(\mathbf{M}_a + \mathbf{M}_c \mathbf{u} - \boldsymbol{\omega} \times \mathbf{J}\boldsymbol{\omega}) \right) (\mathbf{u} - \mathbf{u}_0) \quad (16)$$

The flight test and fly-by-wire system in the aircraft performs data acquisition at 1000 Hz, and the control implementation uses

the same data rate, making the time increments are relatively small. This fact, combined with assuming instantaneous control effectors ($\omega - \omega_0 \ll u - u_0$) and assuming $\omega - \omega_0 = 0$, leads to a simplification of Equation 16 to the following expression where $\Delta u = u - u_0$:

$$\dot{\omega} \simeq \dot{\omega}_0 + J^{-1}M_c \Delta u \quad (17)$$

Inversion of Equation 17 leads to the INDI control law as implemented in the controller. This results in the following where the input of the linear controller v_e replaces $\dot{\omega}$ and the current control surface deflections δ_0 are added. A schematic overview is given in Figure 2:

$$u = M_c^{-1}J(v_e - \dot{\omega}_0) + \delta_0 \quad (18)$$

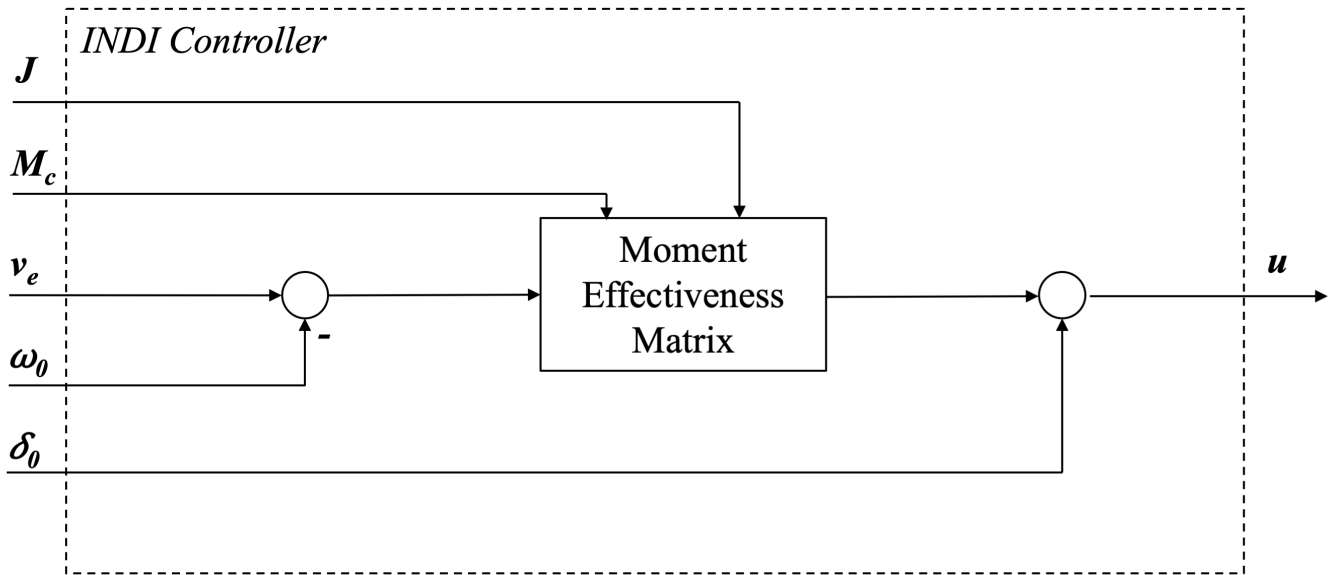


Fig. 2 Schematic block diagram of the INDI controller

2. System Dynamics

The system dynamics are based on the DASMAT model of the Cessna Citation 500 described by Borst [33]. Although developed for another variant, the DASMAT model is preferred over a newer Cessna Citation II model developed by Van den Hoek et al. [34], since it also includes models for the moments of the trim tabs. These moments are relevant when the model has to be trimmed towards steady, straight flight with the lowest possible hinge moment in the elevator. This low hinge moment in the elevator is needed to maximize the performance of the limited fly-by-wire system.

The non-linear actuator model from Lubbers [14] is implemented in this DASMAT model. An alternative to this non-linear actuator model is based on a first-order approximation performed by Grondman et al. [13]. To be able to use both the non-linear

actuator model and a more basic approximation of the actuators, both are modeled and a switch is added to select the used model. Grondman's model has been extended to make use of the saturation flags from the full actuator model by Lubbers [14], to ensure the appropriate saturation deflections.

During the flight test experiment, the DASMAT model is still used to determine the moment induced by the control effectors. However, the mass model has been updated to include the appropriate inertia's and masses from the Citation II. The outputs from the aircraft sensors are synchronized and filtered using basic first-order low-pass filters, except for the angular acceleration which is filtered using a second-order low-pass filter ($\omega = 20$ [rad/s] and $\zeta = 1$). These outputs are used in the remainder of the controller.

IV. Offline Simulation

Multiple offline simulations were performed to investigate the performance of the controller. These simulations used the DASMAT model, in combination with a model for the actuator hardware and the control structure described above. The offline simulations were used to determine the optimal flight condition considering the moment effectiveness and actuator saturation. This led to an initial estimation of the system limitations.

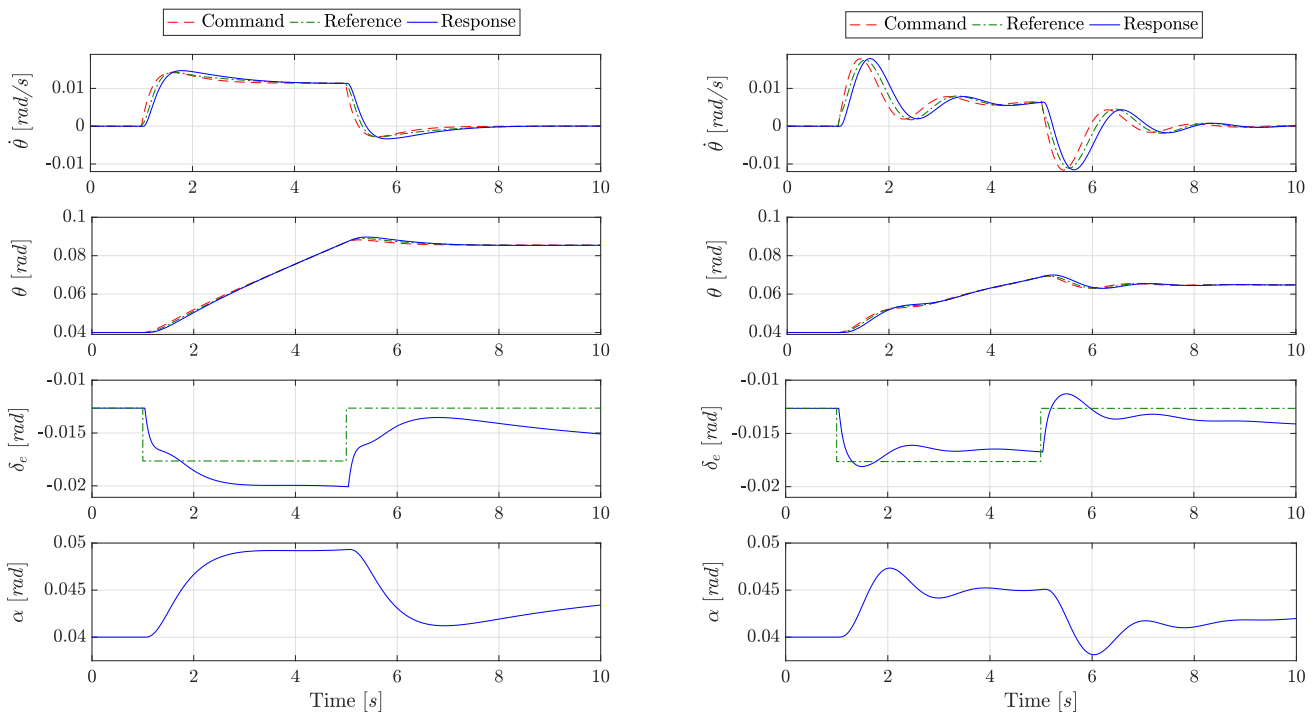
A. CAP and damping performance

To investigate the performance in placing the CAP and damping parameters, step inputs were given on the pitch axis in Figure 3. The same step input is given in both situations, but the settings for the CAP reference model are different. Figure 3a shows the response of the aircraft for a CAP of 0.6 and a damping of 1.0. Figure 3b depicts the response for a CAP of 1.1 and a damping of 0.3. The controller modifies the response of the elevator to match the requested dynamics as closely as possible. In both cases the PCH is enabled, which results in the difference between the commanded signal and the reference signal.

The matching performance of the PCH depends on a proper synchronization of the signals. A transport lag exists between the commanded deflection and the actual deflection of the actuators, which resulted in an over-correction by the hedging signal. During the offline simulations and the fixed-base experiment this transport lag is relatively constant, but in real flight this lag may vary due to various non-linearities. An option was added to the experimental interface to tune the signal synchronization to account for this lag. In addition, the hedging signal directly adapts the CAP reference model, causing a handling qualities change when PCH is enabled, which is undesired behavior. This change should be taken into account when using PCH in the flight tests.

B. Flight condition

The offline model was used to investigate the initial flight condition that would result in the highest pitch and roll rates. This condition was limited by two main factors, being the moment effectiveness and the deflection of the actuators. The moment effectiveness is higher for high speeds and low altitudes, whereas the maximum deflection of the actuators is higher at low speeds and high altitudes. A controller in the fly-by-wire system allows command over the deflection angle of the control surfaces, by controlling the servo motor position. The transmission ratio between deflection of the control surface and position of the servo motor is not a fixed ratio, however, it depends on the force on the actuator cables due to cable stretch. The control effectiveness



(a) CAP = 0.6; Damping = 1.0

(b) CAP = 1.1; Damping = 0.3

Fig. 3 Aircraft pitch response for different CAP and damping values, with PCH enabled

therefore changes dependent on the flight condition. Combining these factors led to an initial condition of 4,000 [m] altitude and a true airspeed of 110 [m/s]. At altitudes higher than approximately 4,250 [m], torque limiters are active for the fly-by-wire system. This was one of the main limiting factors when determining the optimal initial condition with respect to system performance.

C. System limit prediction

To determine the CAP and damping limits of the system, it is necessary to make an assumption regarding the time it takes before pilots experience differences in handling qualities due to actuator saturation. In addition, this is dependent on the behavior of the pilot during the experiment. Some pilots might fly the aircraft with a higher gain, which results in different crossover frequencies and actuator use. The effect of both parameters on the system limits is investigated. Off-line analysis found the crossover frequency has a considerable impact on the system limits, due to the actuator saturation occurring more frequently and for a longer time when the modeled crossover frequency is higher. For the initial system limit prediction it is assumed pilots feel a difference in handling qualities when actuator saturation of 0.2 seconds or longer occurs. This assumption will be updated after the simulator experiment, since this gives an opportunity to investigate a relation between experienced handling qualities and the actuator saturation.

Using a pilot model with different crossover frequencies it was investigated for which combinations of CAP and damping actuator saturation of 0.2 seconds would occur for the control task of the fixed-base simulator experiment. Figure 4 illustrates the effect of two different crossover frequencies as a function of CAP and damping ratio for the defined control task. The pink dots represent the initial conditions chosen for the simulator experiment, which will be explained in more detail below.

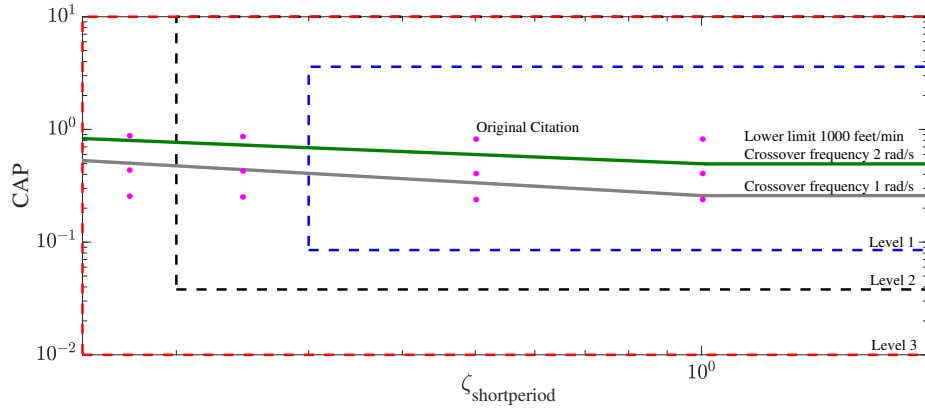


Fig. 4 Initial conditions displayed with predicted limitations from offline simulation

V. Experiment 1: Fixed-base Simulator

A fixed-base simulator experiment is performed to investigate what the system limits are due to the actuator saturation for a specific control task. In addition, it is investigated whether pilots can feel the difference between simulating just the reference model, and simulating the complete non-linear dynamics of the reference model, controller and aircraft.

A. Method

1. Apparatus

The experiment was performed in a fixed-base, part-task flight simulator at Delft University of Technology's Human Machine Interaction Laboratory (HMI lab). Figure 5 depicts the layout of the aircraft configuration. It uses an adjustable aircraft seat, two 18 inch LCD panels that show the instrumentation and three DLP projectors which are used to display the outside visuals. Participants used an electro-hydraulic side stick to control the motion in pitch and roll. Clouds were added to the simulation to enhance the experience of forward motion for the pilots.

2. Software

Since multiple experiments were performed on different platforms, DUECA is used as the main software platform [35]. DUECA has been developed to act as a middleware layer between hardware (simulators/research aircraft) and the actual control software itself. The Matlab/Simulink implementations of the control laws and of the DASMAT model including modeling of the actuators were converted to C code through code generation and integrated in a DUECA project. DUECA provides a scripting interface and publish-subscribe mechanisms to select which parts of the software need to be run, by which the same software project could be deployed both in the simulator and on the Cessna Citation II laboratory aircraft.



Fig. 5 Fixed-base simulator in aircraft configuration

3. Subjects and Instruction to Subjects

Eight pilots participated in the experiment (Table 2). They were instructed to control the aircraft's rate of climb to 1,000 [feet/min] and $-1,000$ [feet/min] (± 5.08 [m/s]), with a performance band around the commanded rate of climb of 10%. Every ten seconds they were commanded to switch between ascent and descent.

4. Independent Variables

The experiment had one independent variable: the model the pilot is using to fly the simulation. Two models were flown: the reference model and the full model. The reference model (CAPR) uses the response from the CAP reference model and sends these dynamics directly to the simulator. The full model (FULL) also includes the controller and the aircraft dynamics. This is represented in the block diagram in Figure 6. The CAP reference model is not limited by actuator saturation, whereas the full model includes these limitations.

Table 2 Characteristics of the pilot subjects

Pilot	Age	Gender	Hours	Types of aircraft
A	52	M	12,000	Single engine; B777; B787; Cessna Citation II (1,000h)
B	63	M	20,000	Single engine; B777; B787; Cessna Citation I (500h)
C	59	M	3,700	Single engine; F5; F16
D	65	M	22,000	Single engine; B737; B747; Cessna Citation I (50h)
E	42	M	3,700	Single engine; Cessna Citation II (1,650h)
F	46	M	2,200	Single engine; SA266/277; Cessna Citation II (1,300h)
G	58	M	14,300	Single engine; Jet engine; Cessna Citation II (3,000h)
H	52	M	1,300	Single engine; Jet engine; Cessna Citation II (6h)

5. Experimental Design and Procedure

The experiment was designed to be full-factorial within-subjects. The CAP conditions were selected to ensure that different system limitations, due to actuator saturation, could be experienced. This resulted in a CAP of 0.90, 0.45 and 0.25.

The different damping conditions were selected to have all three levels of acceptability in the experiment. The original damping of the Cessna Citation II was also included and this resulted in a damping of 0.15, 0.25, 0.5 and 1.0. Combined with the initial CAP conditions, this yielded 12 conditions which are represented by the pink dots in Figure 4.

The initial conditions were flown for both the CAP reference model and the full model, resulting in a total of 24 runs. The 24 runs were divided into 4 sets of 6 runs, where for every set the damping coefficient remained constant, whilst the CAP and simulation model varied. Before every set, training runs were performed to suppress learning effects. These training runs were performed on the settings of the first run of the upcoming set. An example experiment schedule, for one pilot, is shown in Table 3. Sets were varied over all pilots, including the start with the full or CAP reference model per set. The resulting experiment matrix required eight pilots. The initial flight conditions of all runs were defined according to the offline simulation (4,000 [m] altitude and 110 [m/s] true airspeed).

6. Dependent Measures

The dependent measures are used to determine the differences between the conditions of the independent variable. In addition, they are also used to find the limits of the full model based on actuator saturation. The dependent measures are defined as follows:

- **Cooper-Harper Rating Scale:** The subjects had to give a Cooper-Harper rating after every run. The difference between the CAP reference model and the full model for the same initial condition is used to compare the results.
- **Performance:** The total time spent within the specified 10% bandwidth around the required rate of climb is used as

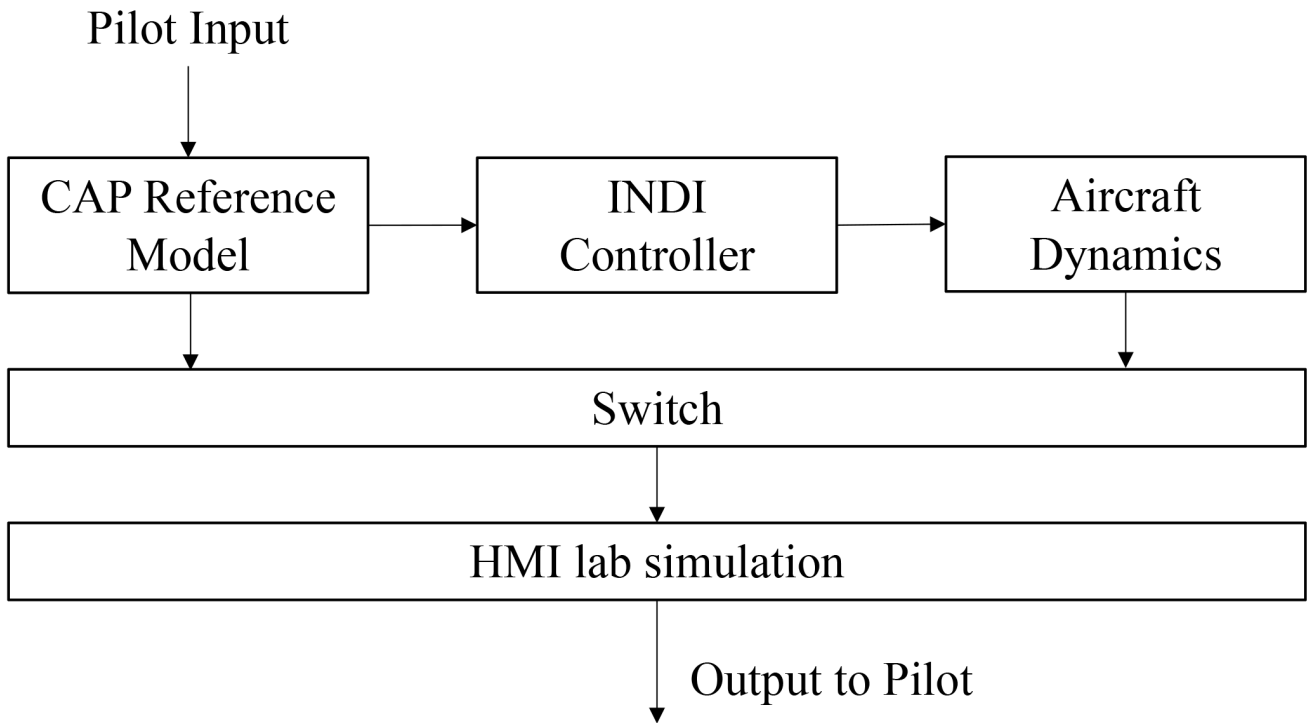


Fig. 6 Flow diagram concerning the independent variable with two conditions

performance indicator. The percentage of the total run time is referred to as the performance ratio.

- **Control activity:** An increased workload indicates the pilot has a harder time flying the aircraft. The control activity during the simulation may therefore be used as workload measure. Control activity is measured by the variance of the input of the pilot. Since the main goal is to determine whether the pilots notice the change in longitudinal handling qualities, only the control activity in pitch is of interest.
- **Actuator saturation:** Actuator saturation is measured since a correlation is expected between the actuator saturation and the differences in Cooper-Harper rating between the different models. Two different flags are used. The first one is logged when actuator saturation occurs and will be referenced as *saturation flag* in the remainder of this paper. The second one is logged when actuator saturation occurs *and* the requested input of the pilot is in the opposite direction of the current aircraft movement. In other words, a pilot might not feel saturation when the aircraft is moving in the direction as requested by the pilot. This flag is referenced to as the *combined flag*.

7. Experiment hypotheses

The following is hypothesized:

- **H.1:** Pilot performance is similar for both models if no actuator saturation is occurring. Performance is expected to be lower if pilots reach the saturation limits of the actuators. Since actuator saturation is expected during the experiment, the full

Table 3 Example of an experiment schedule for one pilot

SET 1 Damp 0.15	SET 2 Damp 0.25	SET 3 Damp 0.50	SET 4 Damp 1.0
CAPR	FULL	CAPR	FULL
CAP 0.9	CAP 0.9	CAP 0.9	CAP 0.9
FULL	CAPR	FULL	CAPR
CAP 0.9	CAP 0.9	CAP 0.9	CAP 0.9
FULL	CAPR	FULL	CAPR
CAP 0.45	CAP 0.45	CAP 0.45	CAP 0.45
CAPR	FULL	CAPR	FULL
CAP 0.45	CAP 0.45	CAP 0.45	CAP 0.45
CAPR	FULL	CAPR	FULL
CAP 0.25	CAP 0.45	CAP 0.25	CAP 0.25
FULL	CAPR	FULL	CAPR
CAP 0.25	CAP 0.45	CAP 0.25	CAP 0.25

model is likely to have lower performance compared to the CAP reference model.

- **H.2:** The control activity is higher for the full model, since the full model includes actuator saturation. This means pilots will sometimes not experience the expected response from the aircraft.
- **H.3:** Pilots will give more similar Cooper-Harper ratings for a higher CAP, since the offline simulation showed actuator saturation time is lower for these conditions. However, this depends on the crossover frequency of the pilot and the assumption pilots only experience differences when a saturation time of more than 0.2 seconds occurs.

B. Results

1. Cooper-Harper difference

The difference in Cooper-Harper rating between both models is displayed in Figure 7. As can be seen, most runs were assessed with two points difference, which means pilots experience the full model to have a worse rating compared to the CAP reference model. For only one run the full model was considered to be the better model. There was a statistically significant difference in Cooper-Harper rating depending on the initial CAP level, $\chi^2(2) = 44.816$, $p < 0.00$. Post hoc analysis was performed using the Wilcoxon signed-rank tests with a Bonferroni correction (significance level of $p < 0.02$). Median perceived Cooper-Harper differences for the CAP of 0.90, 0.45 and 0.25 were 1 (0 to 2), 2 (2 to 4) and 2 (2 to 3.75), respectively. There were significant differences between the CAP 0.90 and 0.45 condition ($Z = -4.247$, $p < 0.00$) and between the CAP of 0.90 and 0.25 ($Z = -4.430$, $p < 0.00$). However, there was no statistically significant reduction in the perceived Cooper-Harper difference between CAP 0.45 and 0.25 ($Z = -0.540$, $p < 0.59$).

The difference in rating can be illustrated using the aircraft response of two experiment runs. Figure 8 shows a run of the full model, where the pilot did not notice any differences compared to the CAP reference model (0 point Cooper-Harper difference). The first subplot shows the rate of climb and the performance bands (marked as two gray boxes). Furthermore, the pitch angle and

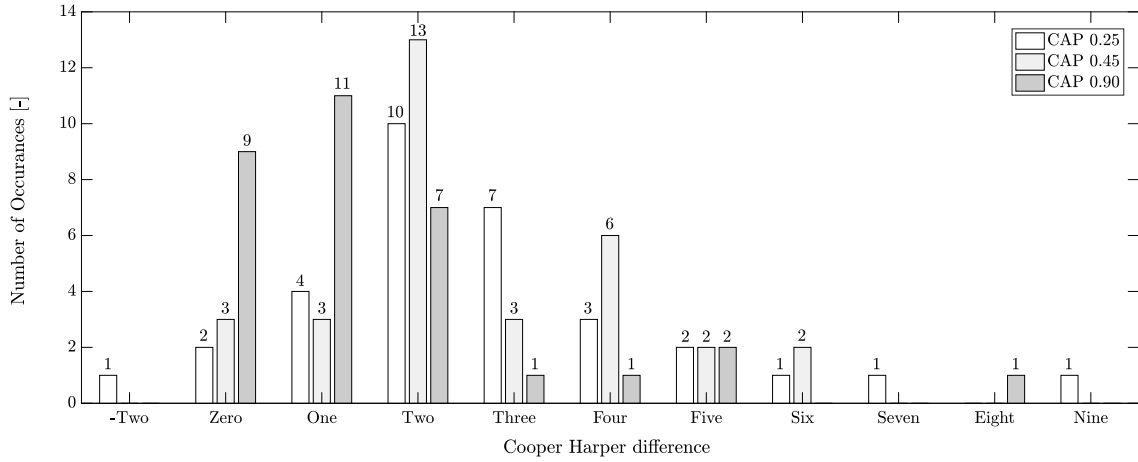


Fig. 7 Cooper-Harper difference between CAP reference model and the Full model as indicated by the pilots

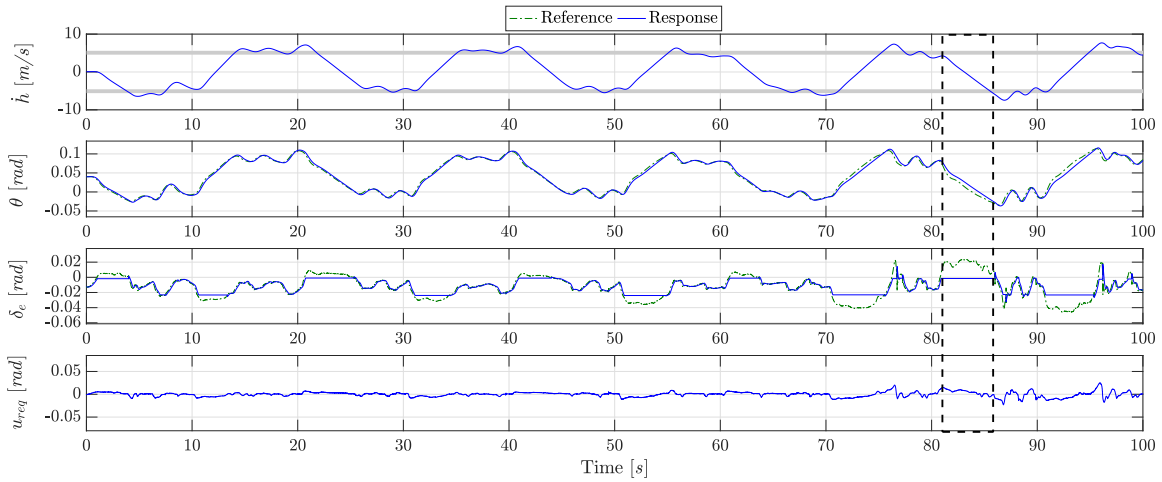


Fig. 8 Aircraft response with Cooper-Harper difference of 0pt (CAP 0.9; Damping ratio 0.25)

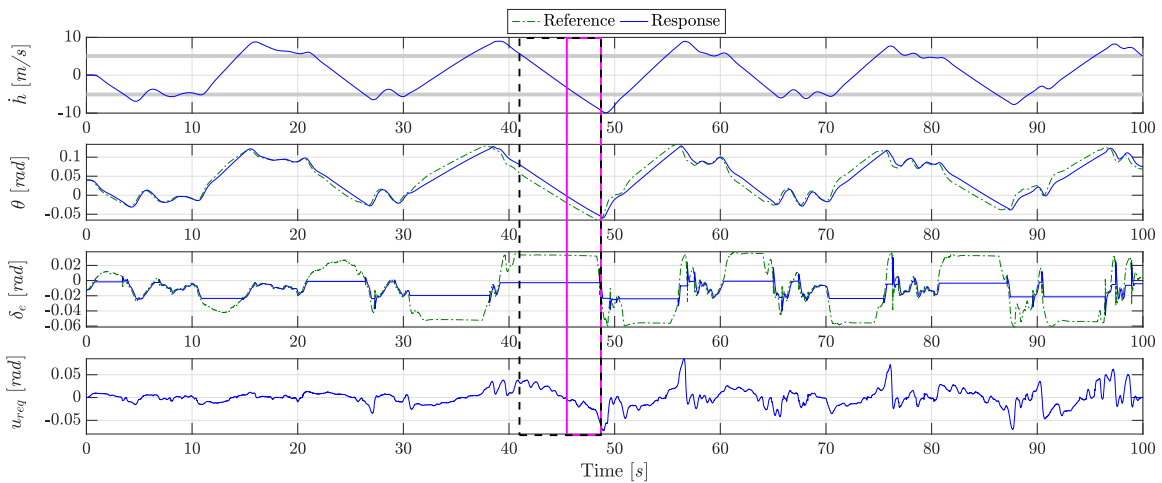


Fig. 9 Aircraft response with Cooper-Harper difference of 6pt (CAP 0.25; Damping ratio 1.0)

elevator deflection are given. Finally, the pilot input is displayed. This shows the longest sustained saturation time occurs in the black dotted box between 80 and 90 seconds (the previously mentioned saturation flag). Even though the model is experiencing saturation, the pilot still graded the full model similar to the CAP reference model.

Figure 9 shows another run of the full model, but here the pilot is noticing a six-point Cooper-Harper rating difference with respect to the CAP reference model. Saturation occurs more often and is sustained for a longer period of time. Like before, the black dotted box between 40 and 50 seconds shows the saturation flag. The magenta box shows the combined flag, during which the pilot tries to steer the aircraft in a different direction, but the aircraft does not respond as requested.

The maximum saturation time for both the saturation flag and the combined flag can be plotted against the Cooper-Harper differences. This can be used to investigate the correlation between the maximum flag time and the difference in experienced handling qualities. The saturation flag is plotted in Figure 10, whereas the combined flag is displayed in Figure 11. The digit behind the summation symbol Σ represents the number of data points in the respective column. The flag time means and standard deviations increase when the perceived Cooper-Harper rating difference increases. The saturation flag appears to have higher means compared to the combined flag. However no statistically significant linear correlation could be found between the Cooper-Harper differences and their corresponding maximum flag time.

2. Statistical Analysis of other dependent measures

Performance of the test subjects using both models is shown in Figure 12. Since the data passed the normality and homogeneity of variance tests, a dependent t-test is performed to evaluate differences. Performance in the full model (0.242 ± 0.052) was significantly lower compared to the CAP reference model (0.268 ± 0.070) with $t(95) = 3.387$ and $p < 0.05$.

Control activity of test subjects using both models is shown in Figure 13. The control activity data did not pass the normality and homogeneity of variance tests. A Wilcoxon signed-rank test is therefore applied to compare the results. This test showed a statistically significant lower control activity with the CAP reference model ($Z = -8.018$ and $p < 0.00$).

The combined flag duration is illustrated in Figure 14, as function of CAP levels. Mauchly's test $\chi^2(2) = 6.225$, $p < 0.04$ indicates the assumption of sphericity is violated. Using a full-factor ANOVA and applying a Greenhouse-Geisser correction determined the mean CAP differed significantly ($F_{1,684} = 6.831$, $p < 0.00$). Post hoc tests with Bonferroni correction (significance level of $p < 0.02$) show the CAP of 0.90 (1.129 ± 2.15) differs significantly from the CAP of 0.25 (2.456 ± 2.54) $p < 0.01$, but there are no significant differences between a CAP of 0.90 and 0.45 (1.964 ± 1.993) $p < 0.03$ and a CAP of 0.45 and 0.25 with $p < 0.49$. However, the difference between a CAP of 0.90 and 0.45 is close to the significance level of $p < 0.02$.

C. Discussion and conclusions

The purpose of the simulator experiment was to identify whether pilots could notice the difference in handling qualities between the CAP reference model and a full aircraft dynamic model including the controller.

The first hypothesis (H.1) is confirmed, since the performance of the pilots was lower for the full model compared to the CAP reference model. When actuator saturation is occurring, it is more difficult for pilots to achieve desired performance.

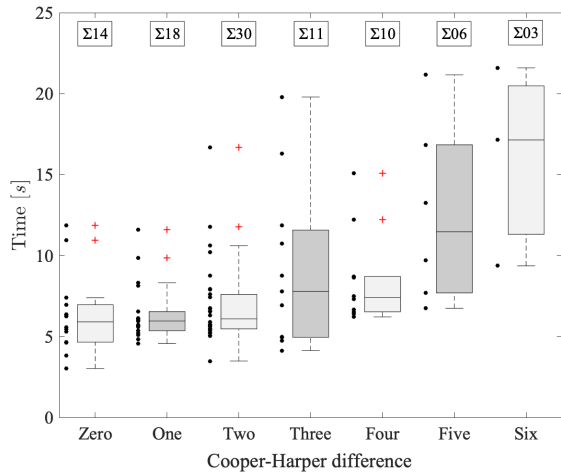


Fig. 10 Means and the 95% confidence limits of the saturation flag sorted by Cooper-Harper difference

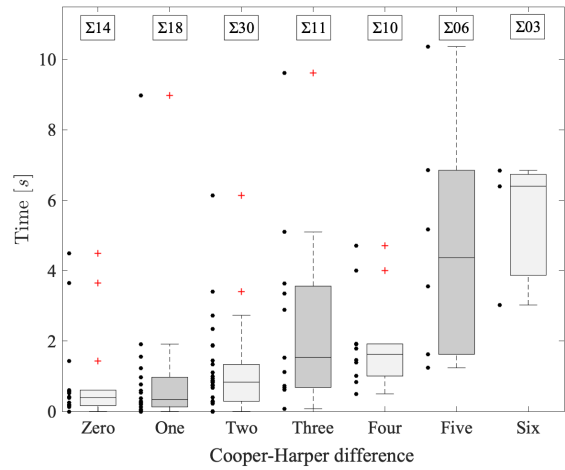


Fig. 11 Means and the 95% confidence limits of the combined flag sorted by Cooper-Harper difference

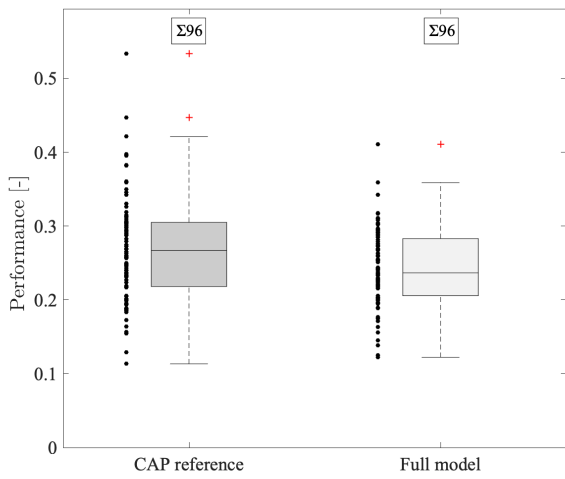


Fig. 12 Means and the 95% confidence limits of the performance

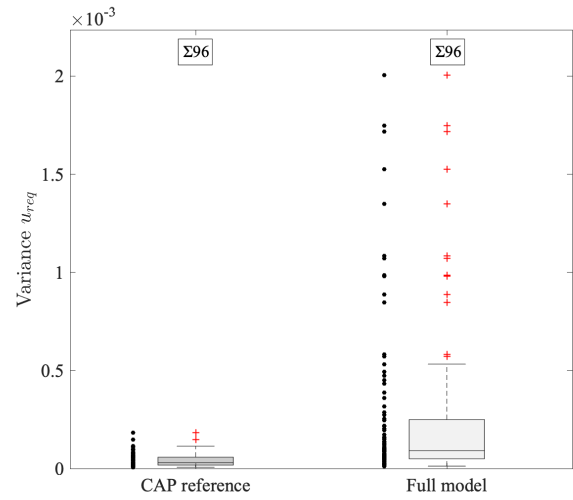


Fig. 13 Means and the 95% confidence limits of the control activity

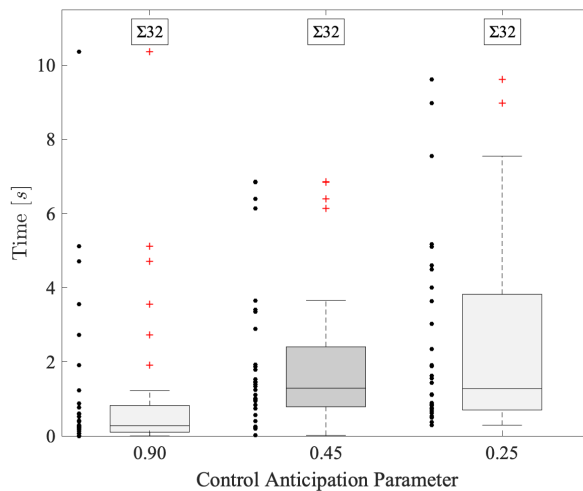


Fig. 14 Means and the 95% confidence limits of the combined flag sorted by CAP

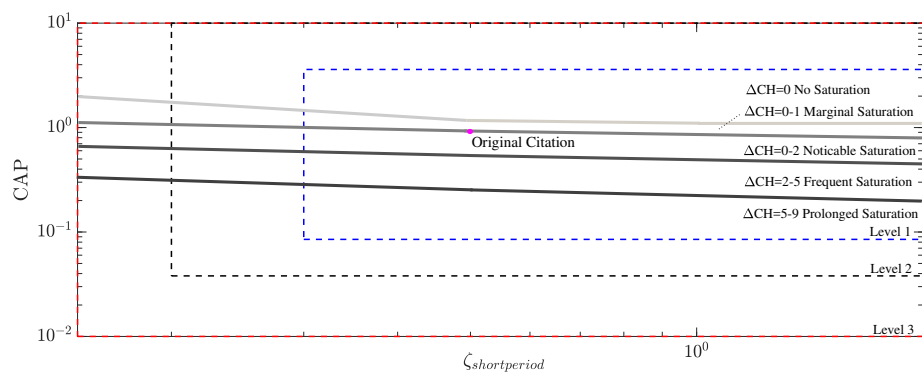


Fig. 15 Updated handling quality limitations using the combined flag saturation information

H.2 is also confirmed. The control activity of the pilots was indeed higher for the full model compared to the CAP reference model. This can be explained by the additional control efforts of pilots that occur when the aircraft does not respond according to their expectations, here mostly due to actuator saturation.

The full model is generally rated at a lower Cooper-Harper rating compared to the CAP reference model. This relates to the difference in response between the models in case of actuator saturation. In addition, some lag is present within the full model due to the actuator dynamics (requested deflection by the pilot is not instantly the actual deflection), whereas this lag is not present in the CAP reference model. At CAP values of 0.90 the mean difference between the experienced handling qualities was on average only 1 Cooper-Harper rating point, whereas this difference increased for lower CAP values with increased actuator saturation. This confirms H.3, since the model mismatch was higher for CAP below the lower limits determined in offline simulation.

The relation between saturation duration and pilots' reported handling qualities was investigated. However, differences in Cooper-Harper rating appear not to be directly related to the flag time. Additional runs would be required to investigate this in more detail. The lower limits obtained with the offline simulations (Figure 4) are updated with the acquired saturation time information as shown in Figure 15. The updated estimation includes the expected Cooper-Harper differences for specific CAP and damping settings for this control task. The updated simulation model can be used for different control tasks to investigate the limits of the full system.

VI. Experiment 2: Flight Test

To validate the controller design and implementation, four flight tests were performed over the course of eight days. The flights all departed from and terminated at Amsterdam Schiphol Airport (AMS) and were flown in the TMA Delta and above the North Sea, within the Netherlands Airspace. The system is validated using the three initial flight tests, whereas the final flight was a demonstration flight.

A. Method

1. Apparatus

The Cessna Citation II laboratory aircraft, jointly operated by TU Delft and the Netherlands Aerospace Centre, was used in the flight tests. The flight tests are performed in a clean configuration with spoilers, gear and flaps retracted. The angle of attack and side slip are measured in clean air using a boom mounted in front of the aircraft. Activation of the automatic trim would disrupt the experimental control system, therefore the trim was deactivated. The aircraft was controlled by the co-pilot, sitting on the right-hand side, using force input on a side-stick. The captain acted as the safety pilot. The experimenter controlled the software and its variable stability settings via a wireless connection using a laptop in the cabin.

The aircraft is equipped with a PC-based data acquisition and a fly-by-wire system that uses the autopilot actuators with modified autopilot hardware to provide experimental control of the aircraft. Through clutches the three autopilot actuators can be mechanically coupled to the mechanical flight control system. The safety pilot uses the mechanical flight control system as the

back-up control, and can use the autopilot disconnect switch to disarm the experimental system. The fly-by-wire hardware and set-up is the same as described in [15], the computer and data acquisition hardware is since renewed, and now uses a quad-core Intel i5 processor. Since data acquisition for analog signals was easily feasible at 1000 Hz, this rate was selected and pre-sample filters were tuned to match this sample rate. The aircraft's ARINC data are read from 18 available ARINC busses, with inertial measurement data being sent at a rate of 52 Hz. Control surface positions are measured with synchros, sampled at 100 Hz, control and measurement of the autopilot actuators runs at 1000 Hz.

2. Changes to controller

Multiple changes were made to the controller with respect to the simulator version. The citation model system dynamics were modified to follow the state given by flight measurements and changed to ensure they only output the moment effectiveness matrix. All other outputs were received from sensors based on the aircraft itself. The requested deflection that comes from the INDI controller was linked to the autopilot servos from the existing aircraft fly-by-wire system [15].

New angular accelerometers were installed on the Cessna Citation II laboratory aircraft. These were an addition to the previously available angular accelerations which were established by differentiating the angular rates. Second order filters were introduced to these angular accelerations to remove noise whilst still maintaining the original signal without too much lag.

The controller required a conversion of the stick gains, since the stick on the aircraft was not identical to the electro-hydraulic stick used in the simulator. The stick on the aircraft converted the input from the pilots to a different scale, thus the gains were adapted to maintain the same scaling (in command input per stick force) as in the simulator.

In comparison to the fixed initial conditions in the fixed-based simulator, the initial conditions depend on the actual flight conditions upon experiment initiation. The updated initial conditions were also used in the determination of the moment effectiveness matrix.

The fixed-base simulator experiment was based on the DASMAT model, which consisted of an inertia tensor based on the Cessna Citation I. Since the experiment is conducted in the Cessna Citation II, it was required to update this inertia tensor based on the newly developed model by Van den Hoek et al. [34]. The model mismatch between the DASMAT model and the new model was highest for the inertia around the y-axis I_{yy} , with a 35% change. The I_{xx} , I_{zz} and I_{xz} showed an increase of 8%, 24% and 27%, respectively.

3. Procedure

The experiments in pitch focused mainly on the longitudinal handling qualities, similar to the experiment in the simulator. In addition, a number of roll maneuvers were performed to test the differences in roll time constants. To demonstrate the system potential to be used in pilot training, the effects of roll time constants, stick time delays and stick gains were also investigated.

Two initial conditions were used during the different flight tests. Both conditions were at an altitude of FL130 (approximately 4000 [m]), but with a varying airspeed of 175 or 190 knots, 97 [m/s] respectively 105 [m/s]. To ensure safe execution of the experiment, the following procedure was used during the experiments. First, the safety pilot flew to the requested altitude. Then he

trimmed the aircraft for the desired airspeed in horizontal flight and disabled the auto trim. At the same time, the experimenter selected the desired parameter configuration in the DUECA software. Activation of the autopilot based on the controller software required activation of both the roll and pitch axes. This was achieved by a trigger of both the safety pilot and the experimenter, for each axis. Finally, the experimental control mode was initiated by the co-pilot, with “hands-off-stick” to prevent undesirable initial control inputs.

4. Subjects and Instruction to Subjects

To validate the controller by noticing the differences in handling qualities, pilots require experience on the Cessna Citation II laboratory aircraft. Three pilots have flown the aircraft in the experiments, being pilots E, F and G (Table 2). In contrast to the fixed-based simulator experiments, pilots did not assign Cooper-Harper ratings, due to the limited number of experimental runs.

Pilots received instructions for the different phases in flight. In accordance with the simulator task, pilots were instructed to fly at $\pm 1,000$ [feet/min] (± 5.08 [m/s]) rate of climb during the test. However, the pilot was free to decide between ascent and descent, as long as the aircraft remains below FL135 (4150 [m]). This restriction was required, as a significant reduction of torque in the fly-by-wire system is activated above FL135.

B. Results

1. Longitudinal response

The longitudinal tracking response of the controller can be seen in Figure 16, where the time on the horizontal axis represents the time passed after starting the controller in the aircraft. The pilot was requested to fly similar maneuvers as in the simulator experiment. The controller was set with a CAP of 0.90 and a damping of 0.50 before 1,160 seconds. After 1,160 seconds the damping was changed to 0.15, whereas the CAP remained the same (indicated by the vertical black dotted line). The reference signal could not be followed properly at some time instants, since the elevator servo was saturated. This is indicated by the current in the actuator servo, I , which reaches the edges of the bandwidth (indicated by the horizontal black dotted lines). This is most visible at the 1,260 seconds time point. In addition, some oscillations (which could be characterized as pilot-induced) were present for lower damping conditions. This is especially evident when comparing the pilot input to the reference signal between 1,270 and 1,300 seconds. The pilot also noticed this PIO himself when flying the aircraft. The lower damping was also identified by the pilot. The maximum $\Delta\delta_e$ during this run equaled $1.76 \cdot 10^{-3}$ [rad] or 1.01 [deg], whereas the maximum requested deflection by the controller equaled $3.91 \cdot 10^{-2}$ [rad] or 2.24 [deg].

The aircraft was properly trimmed before the run shown in Figure 16. The impact of improper trim is illustrated in Figure 17. Some maneuvers were performed before the start of this run, which resulted in a mismatch between the trimmed and actual indicated airspeed of ≈ 10 [m/s]. The effect is seen in the actuator servo current I , where the initial value is not close to zero as indicated by the black line (in contrast to Figure 16). Additional actuator deflection was required to remain straight and steady flight at this higher speed, resulting in a nonzero current. The available bandwidth above the black line is smaller compared to the

bandwidth below. This resulted in more actuator saturation and a lower maximum elevator deflection. Pilots indeed noticed this effect during flight, saying it was easier to control the aircraft in one direction compared to the other when the aircraft was not properly trimmed. A change of indicated airspeed of more than 5 [m/s] already resulted in this effect, according to the pilots. In addition, pilots noticed the handling qualities of the aircraft were better when a lower pilot gain was used. This is confirmed in Figure 17, since higher stick deflections by the pilot result in more actuator saturation. The maximum $\Delta\delta_e$ during this run equaled

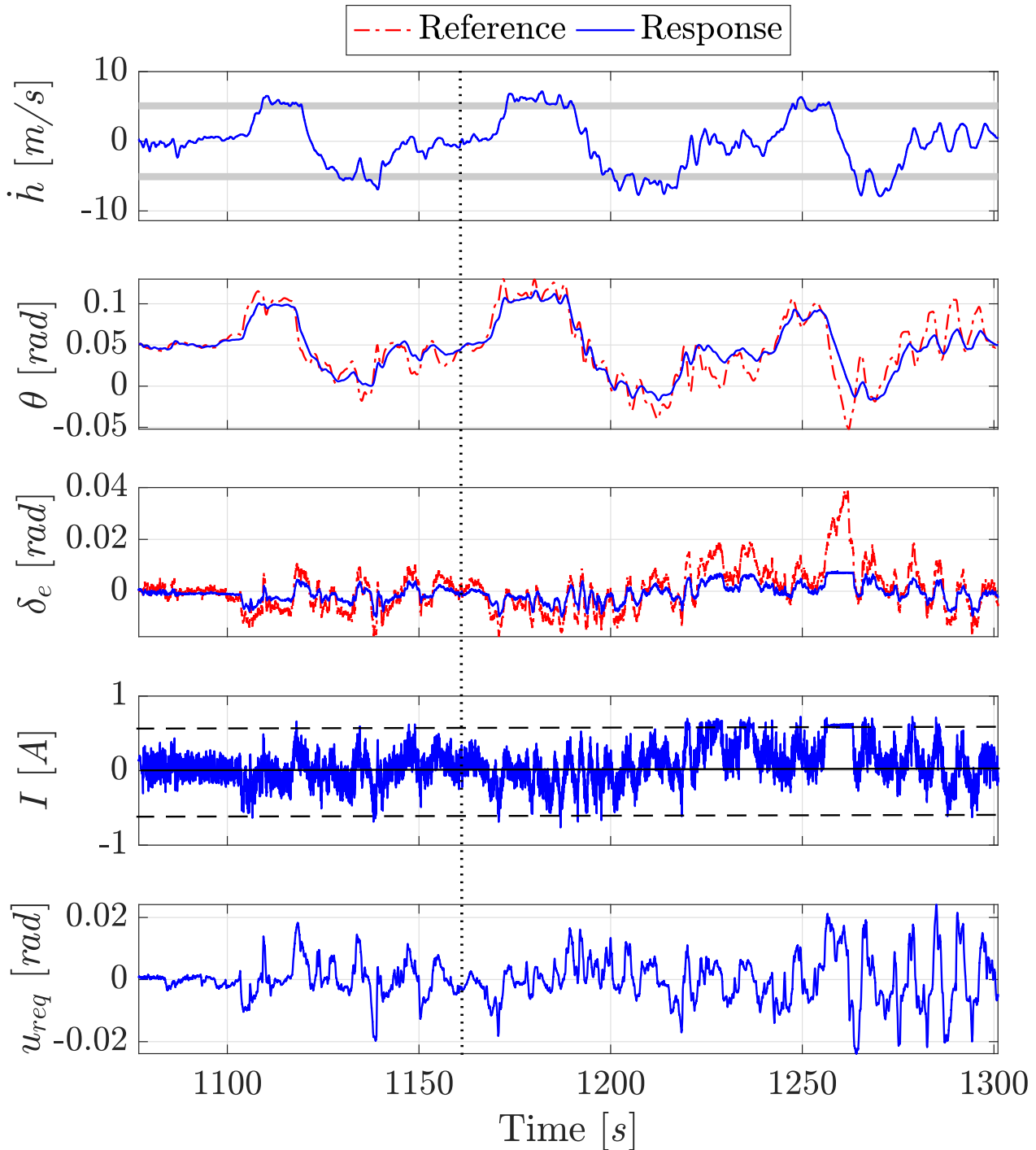


Fig. 16 Longitudinal tracking response ($V_{ias} = 110$ [m/s] FL130)

$1.61 \cdot 10^{-3}$ [rad] or 0.917 [deg], whereas the maximum requested deflection by the controller equaled $1.43 \cdot 10^{-1}$ [rad] or 8.08 [deg].

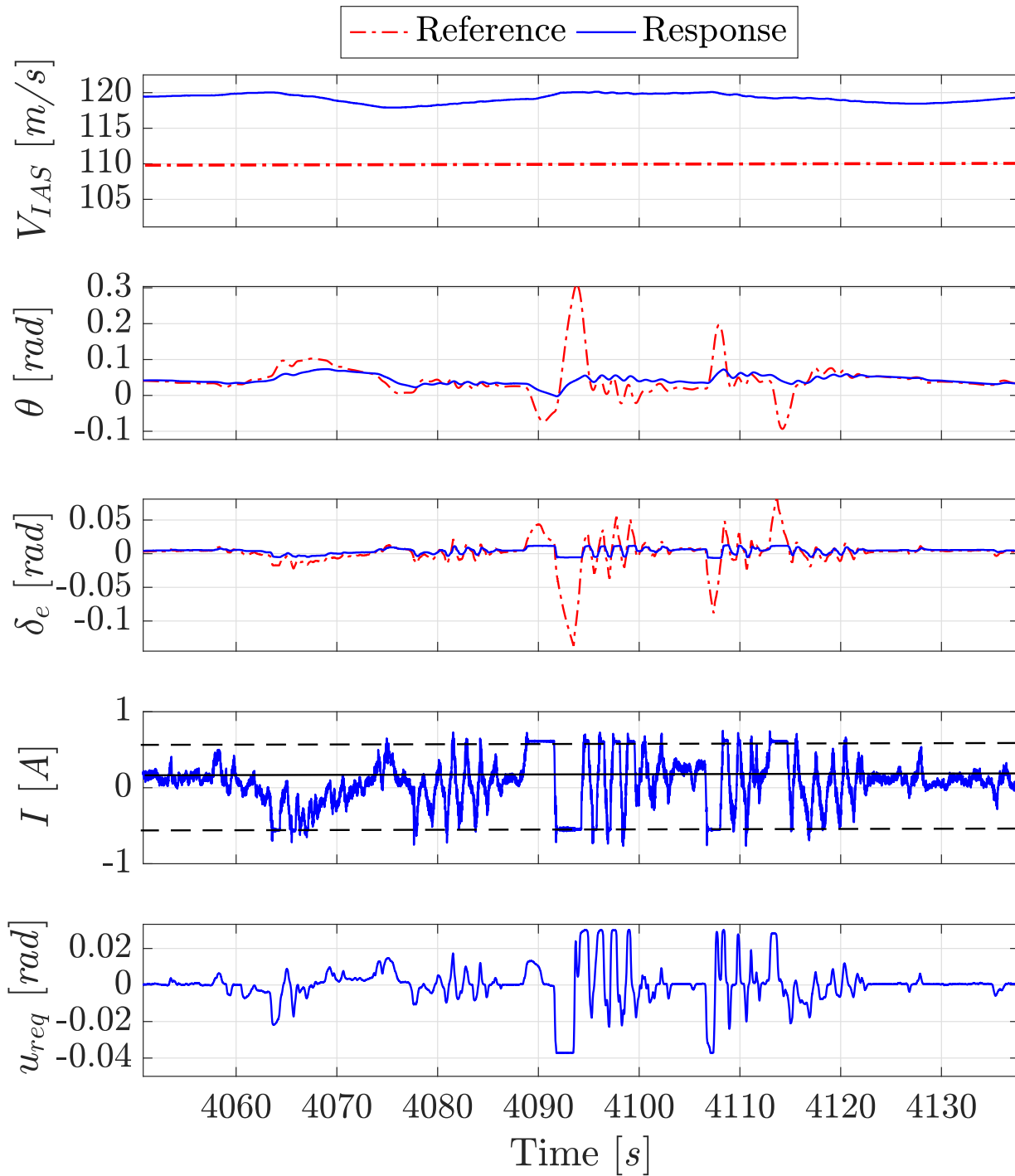


Fig. 17 Longitudinal tracking response ($V_{ias} = 120$ [m/s] FL130)

C. Discussion and conclusions

Four flight tests were conducted to validate the variable stability controller. During the third and fourth flight test, the pilots noted the response of the controller and the aircraft was similar to the experiment in the fixed-base simulator. This is confirmed by the comparison between the reference dynamics and the actual response of the aircraft. Due to time and cost limitations, the simulator experiment could not be exactly reproduced in the real flight test. However, pilots commented they could notice differences between different damping settings, similar to the experiment in the fixed-base simulator.

The system limitations were identified by pushing the system in roll and pitch whilst deviating from the initial trim condition. When the aircraft was within the performance bandwidth of the actuator servos, the INDI controller was able to track the reference signal quite well. It is expected this can be further improved by implementing the aerodynamic model from the Cessna Citation II by Van den Hoek et al. [34], since the controller currently uses the aerodynamic model from the Citation I.

Actuator saturation is considered to be the most limiting factor, since tracking performance significantly decreases when saturation occurs. The requested deflection by the controller was in extreme cases both for the pitch as roll axis higher than the actual saturated deflection, by a factor of 8-10 in pitch and 3-4 in roll, respectively. This is by far the most limiting factor of the variable stability system performance. Given limited time on the flight test campaign the Pseudo-Control Hedging mode was not further tuned and tested.

The most obvious solution to the limitations would be to replace the current fly-by-wire system with a more powerful system. This is however an expensive hardware change which requires re-certification. A possible improvement of the current system can be achieved by adding control of the elevator trim in the control laws. Future research should investigate whether a lower hinge moment can be achieved using the auto trim, without interfering with the actual response of the elevator. This could increase the performance band of the system in longitudinal motion but would also require hardware changes to the aircraft. Another solution would be to keep the auto trim activated and use the software model to predict when the auto trim is going to occur. This could then be used to minimize the interference of the auto trim on the actuator deflection. However, the expected non-linearities during flight limit the accuracy of any auto trim function predictions. This method is therefore considered a complicated alternative.

VII. Discussion and Recommendations

The purpose of this paper was twofold. First it was investigated whether an INDI controller can be used to create a variable stability in-flight simulator. Second, the limitations of the resulting system were researched. The controller was tested in offline simulations, during a fixed-base simulator experiment and in actual flight tests.

A. Handling qualities

The INDI technique is able to implement inner loop control for a handling qualities reference model in a variable stability system. Offline simulations showed the controller manipulates the response of the actuators to ensure tracking performance of the CAP reference model. The flight condition that provides the best performance for the Cessna Citation II laboratory aircraft was determined to be at 4,000 [m] altitude with a true airspeed of 110 [m/s]. PCH improved the controller performance by slightly

modifying the CAP reference signal when there was no actuator saturation present. However, the hedging signal adapted the CAP reference model more significantly when the actuators were saturating. This implies the handling qualities change when PCH is enabled, which is undesired behavior.

An experiment was performed in a fixed-base simulator to determine whether pilots could notice the difference between the CAP reference model and a full model including the aircraft and actuator dynamics. The control activity of the pilots was higher for the full model compared to the CAP reference model, and the performance of the pilots was lower for the full model. These can both be explained by pilots who are not experiencing the expected response of the aircraft when actuators are saturating.

A vertical speed capture task was used by the pilots to evaluate the handling qualities. Pilots rated the full model on average two Cooper-Harper points lower compared to the reference dynamics model, which is hypothesized to occur due to actuator saturation. This was indeed confirmed by the differences of rating for the different CAP conditions. The CAP of 0.90 was rated at a mean Cooper-Harper difference of one, which differed statistically from the CAP of 0.45 and 0.25 with a mean Cooper-Harper difference of two. The CAP of 0.90 also showed a shorter maximum saturation time compared to the CAP of 0.25, whereas the difference between CAP 0.90 and 0.45 was close to the significance level. This confirmed the initial estimation of the system limitations. The actuator saturation data were compared with the Cooper-Harper differences between the CAP reference and the full model. The saturation time was used to update the model for estimating the handling quality limitations.

Flight tests were performed to validate the performance of the controller. In response to changes in the reference model settings, pilots noted they experienced the changes in CAP and damping similar to those found the fixed-base simulator experiment. However, they also experienced some limitations to the system, most likely related to actuator saturation with larger inputs and conditions that deviated more from the base aircraft dynamics.

B. System limitations

Two factors were found to be limiting for the variable stability in-flight simulator using the INDI technique. The first factor was the accuracy of the moment effectiveness parameter. This parameter depends on the accuracy of both the aerodynamic coefficients and the aircraft inertia. During the offline simulations and the fixed-base experiment the controller showed proper tracking performance. Even in the flight tests, when additional non-linearities and disturbances are present, the INDI controller could track the reference model properly. This can be further improved, however, by updating the aerodynamic coefficients to the newer Cessna Citation II model.

The second and most limiting factor was found to be the actuator saturation. The tracking performance of the controller decreased significantly when actuator saturation occurred. Saturation occurred either when the input of the pilot was too high, or when the aircraft deviated too much from its initial trim condition. The maximum deflection of the elevator was approximately 1 [deg], whereas the maximum deflection of the ailerons was around 6 [deg]. These limited deflections arose from the constraints of the fly-by-wire system. Future research should investigate whether a lower hinge moment can be achieved using the auto trim, without interfering with the actual position of the elevator. This could increase the performance band of the system in longitudinal motion but would also require hardware changes to the aircraft.

The hardware set-up shared the high sampling and data rate inherited from the basic flight test instrumentation system from which it is derived. While the high update rate is convenient in this application, it is not feasible to expect that standard flight hardware will be able to run at this data rate. Given the required control bandwidth and the dynamics of actuators and the aircraft, it is expected that the system can also be operated at lower update rate, which would require additional (digital) filtering in our set-up. Investigation of the effect of update rate on the controller performance would be recommendable in that case.

A further improvement for the system relates to the noise generated in the differentiation step needed to derive angular acceleration values. Possible improvements for this step are the application of sliding mode differentiation [36].

The current implementation had a flaw in the formulation of the lateral reference model, invalidating the results for lateral motions. The lateral control was stable, and did not interfere with the tests in longitudinal control.

VIII. Conclusions

This paper investigated whether the Cessna Citation II can be converted in a variable stability system, using Incremental Non-linear Dynamic Inversion (INDI). Offline simulations show INDI can indeed be used to achieve a variable stability platform. Pseudo-Control Hedging (PCH) increases the controller performance, but also affects the handling qualities. The simulator experiment showed pilots could feel differences between the reference dynamics and a full model including actuators and the INDI controller. Pilots rate the full model on average two Cooper-Harper points lower compared to the reference dynamics model. The experienced model mismatch was higher for Control Anticipation Parameter (CAP) values below the lower system limits as determined in the offline simulation, and actuator saturation increased for lower CAPs.

Four flight tests were conducted to validate the variable stability INDI controller in real flight. Pilots commented they could notice differences between different damping settings, similar to the simulator experiment. System limitations were identified by pushing the system in roll and pitch whilst deviating from the initial trim condition. Especially the longitudinal motion was considered to be limited due to actuator saturation, which poses the main constraint on the developed system.

IX. Acknowledgements

The authors would like to thank the involved staff from the Delft University of Technology: Hans Mulder, Alexander in 't Veld, Menno Klaassen, Ferdinand Postema and Gijsbert den Toom. Their support, guidance and additional time during the project and especially the flight tests was highly appreciated. Finally, the authors would like to thank all pilots who participated in the experiments.

References

- [1] Weingarten, N. C., "History of In-Flight Simulation at General Dynamics," *Journal of Aircraft*, Vol. 42, No. 2, 2005, pp. 290–298. doi:10.2514/1.4663.
- [2] Hamel, P., *In-Flight Simulators and Fly-by-Wire / Light Demonstrators*, Springer Nature, 2017.

- [3] Mirza, A., Van Paassen, M. M., and Mulder, M., "Simulator Evaluation of a Medium-Cost Variable Stability System for a Business Jet," *Proceedings of the AIAA Guidance, Navigation, and Control Conference*, 2019. doi:10.2514/6.2019-0370.
- [4] Armstrong, E. S., *ORACLS, a design system for linear multivariable control*, Control and systems theory ; v. 10, M. Dekker, New York, 1980.
- [5] O'Brien, M. J., and Broussard, J. R., "'Feedforward Control to Track the Output of a Forced Model." Decision and Control including the 17th Symposium on Adaptive Processes," *IEEE Conference on. IEEE*, 1979, pp. 835–842. doi:10.1109/TAC.1980.1102409.
- [6] Kreindler, E., and Rothschild, D., "Model-Following in Linear-Quadratic Optimization," *American Institute of Aeronautics and Astronautics Journal*, Vol. 14, no. 7, 1976, pp. 835–842. doi:10.2514/3.7160.
- [7] Slotine, J. J. E., and Li, W., *Applied Nonlinear Control*, Englewood Cliffs, N.J.: Prentice Hall, 1991.
- [8] Ko, J., Lee, H., and Lee, J., "In Flight Simulation for Flight Control Law Evaluation of Fly-by-Wire Aircraft," *Agency for Defense Development, Daejeon, Republic of Korea*, 2004.
- [9] Ko, J., and Park, S., "Variable stability system control law development for in-flight simulation of pitch/roll/yaw rate and normal load," *International Journal of Aeronautical and Space Sciences*, Vol. 15, No. 4, 2014, pp. 412–418. doi:10.5139/IJASS.2014.15.4.412.
- [10] Miller, C., "Nonlinear Dynamic Inversion Baseline Control Law: Architecture and Performance Predictions," *AIAA Guidance, Navigation, and Control Conference*, Guidance, Navigation, and Control and Co-located Conferences, American Institute of Aeronautics and Astronautics, 2011. doi:10.2514/6.2011-6467, URL <https://doi.org/10.2514/6.2011-6467>.
- [11] Smith, P., "A Simplified Approach to Non-linear Dynamic Inversion Based Flight Control," *23rd Atmospheric Flight Mechanics Conference*, 1998. doi:10.2514/6.1998-4461, URL <http://arc.aiaa.org/doi/10.2514/6.1998-4461>.
- [12] Germann, K. P., *T-6A Texan II In-Flight Simulation and Variable Stability System Design*, Mississippi State University, 2006.
- [13] Grondman, F., Looye, G., Kuchar, R. O., Chu, Q. P., and Van Kampen, E., "Design and Flight Testing of Incremental Nonlinear Dynamic Inversion-based Control Laws for a Passenger Aircraft," *2018 AIAA Guidance, Navigation, and Control Conference*, AIAA SciTech Forum, American Institute of Aeronautics and Astronautics, 2018. doi:10.2514/6.2018-0385, URL <https://doi.org/10.2514/6.2018-0385>.
- [14] Lubbers, B., *A Model of the Experimental Fly-By-Wire Flight Control System for the PH-LAB*, Delft University of Technology (unpublished master thesis), 2009.
- [15] Zaal, P., Pool, D. M., in 't Veld, A. C., Postema, F. N., Mulder, M., van Paassen, M. M., and Mulder, J. A., "Design and Certification of a Fly-by-Wire System with Minimal Impact on the Original Flight Controls," *AIAA Guidance, Navigation, and Control Conference*, 2009. doi:10.2514/6.2009-5985, URL <http://arc.aiaa.org/doi/10.2514/6.2009-5985>.
- [16] Nelson, R. C., *Flight Stability and Automatic Control*, McGraw-Hill Education, 1998.
- [17] Bryson, A. E., and Ho, Y. C., *Applied Optimal Control*, Hemisphere, Washington D.C., 1975.
- [18] Ko, J., and Park, S., "Design of a Variable Stability Flight Control System," *KSAS International Journal*, Vol. 9, No. 1, 2008.

- [19] Bacon, B., and Ostroff, A., "Reconfigurable Flight Control using Non-linear Dynamic Inversion with a special Accelerometer Implementation," *AIAA Guidance, Navigation, and Control Conference and Exhibit*, 2000. doi:10.2514/6.2000-4565, URL <http://arc.aiaa.org/doi/10.2514/6.2000-4565>.
- [20] Cox, T., and Cotting, M., "A Generic Inner-Loop Control Law Structure for Six-Degree-of-Freedom Conceptual Aircraft Design," *43rd AIAA Aerospace Sciences Meeting and Exhibit*, Aerospace Sciences Meetings, American Institute of Aeronautics and Astronautics, 2005. doi:10.2514/6.2005-31, URL <https://doi.org/10.2514/6.2005-31>.
- [21] Smeur, E. J. J., Chu, Q. P., and de Croon, G. C. H. E., "Adaptive Incremental Nonlinear Dynamic Inversion for Attitude Control of Micro Air Vehicles," *Journal of Guidance, Control, and Dynamics*, Vol. 39, No. 3, 2016, pp. 450–461. doi:10.2514/1.G001490.
- [22] Smeur, E. J. J., de Croon, G. C. H. E., and Chu, Q. P., "Cascaded Incremental Nonlinear Dynamic Inversion Control for MAV Disturbance Rejection," *Control Engineering Practice*, Vol. 73, 2018, pp. 79–90. doi:10.1016/j.conengprac.2018.01.003.
- [23] Keijzer, T., Looye, G., Chu, Q. P., and Van Kampen, E.-J., "Design and Flight Testing of Incremental Backstepping based Control Laws with Angular Accelerometer Feedback," *AIAA Scitech 2019 Forum*, American Institute of Aeronautics and Astronautics, San Diego, California, 2019. doi:10.2514/6.2019-0129, URL <https://arc.aiaa.org/doi/10.2514/6.2019-0129>.
- [24] Cooper, G. E., and Harper, R. P., "Handling Qualities and Pilot Evaluation," *Journal of Guidance, Control, and Dynamics*, Vol. 9, No. 5, 1986, pp. 515–529. doi:10.2514/3.20142.
- [25] Bihrlé, W., "A Handling Qualities Theory for Precise Flight Path Control," Tech. rep., Air Force Flight Dynamics Laboratory, New York, 1966.
- [26] Standard, *MIL-STD-1797A Requirements for Flying Qualities of Piloted Aircraft*, Department of Defense, 1990.
- [27] Bischoff, D. E., "The Control Anticipation Parameter for Augmented Aircraft," Tech. rep., Naval Air Development Center, Warminster, 1981.
- [28] Di Franco, D. A., "In-flight Investigation of the Effects of Higher-Order Control System Dynamics on Longitudinal Handling Qualities," Tech. rep., Cornell Aeronautic Lab, Buffalo NY, 1968. doi:10.1002/nav.3800080206.
- [29] Hodgkinson, J., LaManna, W. J., and Heyde, J. L., "Handling Qualities of Aircraft with Stability and Control Augmentation Systems - A Fundamental Approach," Vol. 80, 1976, pp. 75–81. doi:10.1017/S0001924000033510.
- [30] Morelli, E. A., *Identification of Low Order System Models From Flight Equivalent Test Data*, NASA Langley Research Center, 2000.
- [31] Johnson, E. N., and Calise, A. J., "Pseudo-Control Hedging : a New Method for Adaptive Control," *Advances in Navigation Guidance and Control Technology Workshop*, 2000. doi:10.1.1.16.4719.
- [32] Lombaerts, T., and Looye, G., "Design and flight testing of manual nonlinear flight control laws," *AIAA Guidance, Navigation, and Control Conference*, American Institute of Aeronautics and Astronautics, Portland, Oregon, 2011. doi:10.2514/6.2011-6469, URL <http://arc.aiaa.org/doi/10.2514/6.2011-6469>.
- [33] Borst, C., *CITAST: Citation Analysis and Simulation Toolkit*, Delft University of Technology, Delft, 2004.

- [34] Van den Hoek, M. A., de Visser, C. C., and Pool, D. M., "Identification of a Cessna Citation II Model Based on Flight Test Data," *Advances in Aerospace Guidance, Navigation and Control*, 2018, pp. 259–277.
- [35] van Paassen, M. M., Stroosma, O., and Delatour, J., "DUECA - Data-driven Activation in Distributed Real-Time Computation," *Modeling and Simulation Technologies Conference, Guidance, Navigation, and Control and Co-located Conferences*, American Institute of Aeronautics and Astronautics, 2000. doi:10.2514/6.2000-4503, URL <https://doi.org/10.2514/6.2000-4503>.
- [36] Edwards, C., and Spurgeon, S. K., "On the development of discontinuous observers," *International Journal of Control*, Vol. 59, No. 5, 1994, pp. 1211–1229. doi:10.1080/00207179408923128, URL <https://www.tandfonline.com/doi/full/10.1080/00207179408923128>.